Biochemical and Biophysical Research Communications 441 (2013) 820–824

Contents lists available at ScienceDirect

Biochemical and Biophysical Research Communications

journal homepage: www.elsevier.com/locate/ybbrc

Detecting ligand interactions with G protein-coupled receptors in real-time on living cells

Bo Xu [a,1], Zohreh Varasteh [b,1], Anna Orlova [b], Karl Andersson [c,d], Dan Larhammar [a], Hanna Björkelund [c,d,*]

[a] Department of Neuroscience, Unit of Pharmacology, Uppsala University, Husargatan 2, 751 24 Uppsala, Sweden
[b] Preclinical PET Platform, Department of Medicinal Chemistry, Uppsala University, Dag Hammarskjöldsv 14C, 751 83 Uppsala, Sweden
[c] Department of Radiology, Oncology, and Radiation Sciences, Unit of Biomedical Radiation Sciences, Rudbeck Laboratory, Uppsala University, 751 85 Uppsala, Sweden
[d] Ridgeview Instruments AB, Skillsta 4, 740 20 Vänge, Sweden

ARTICLE INFO

Article history:
Received 23 October 2013
Available online 6 November 2013

Keywords:
GPCR
Real-time
LigandTracer
Interaction Map
Kinetics
Heterogeneity

ABSTRACT

G protein-coupled receptors (GPCRs) are a large group of receptors of great biological and clinical relevance. Despite this, the tools for a detailed analysis of ligand–GPCR interactions are limited. The aim of this paper was to demonstrate how ligand binding to GPCRs can be followed in real-time on living cells. This was conducted using two model systems, the radiolabeled porcine peptide YY (pPYY) interacting with transfected human Y2 receptor (hY2R) and the bombesin antagonist RM26 binding to the naturally expressed gastrin-releasing peptide receptor (GRPR). By following the interaction over time, the affinity and kinetic properties such as association and dissociation rate were obtained. Additionally, data were analyzed using the Interaction Map method, which can evaluate a real-time binding curve and present the number of parallel interactions contributing to the curve. It was found that pPYY binds very slowly with an estimated time to equilibrium of approximately 12 h. This may be problematic in standard end-point assays where equilibrium is required. The RM26 binding showed signs of heterogeneity, observed as two parallel interactions with unique kinetic properties. In conclusion, measuring binding in real-time using living cells opens up for a better understanding of ligand interactions with GPCRs.

1. Introduction

G-protein coupled receptors (GPCRs) constitute a large class of receptors of great biological importance. Abnormal expression, regulation and function have been linked to many diseases, making them important targets in diagnostic and therapy. The receptors transduce extracellular signals through the membrane via a number of conformational changes, but despite clinical relevance the knowledge about their molecular mechanisms is limited [1,2].

There are several methods to identify compounds that target GPCRs. Ligand-receptor binding assays, such as saturation assays, are widely used methods to determine the ligand-receptor affinity. Other strategies include indirect signaling assays, where binding to GPCRs is instead monitored by following the activity of the downstream signaling pathway. Although much information can be gained from such assays, a general drawback is that the downstream effect will depend on other components present in the cell, making it difficult to generalize results [3,4]. Furthermore, both saturation assays and activity assays are most often end-point measurements, which typically rely on equilibrium being reached during the time of incubation. This has been identified as a potential source of error, since high affinity binders may have equilibration times of many hours [5,6] and protocols with a few hours of incubation are still common.

An alternative to the assays described above is to monitor the ligand-receptor binding in real-time. These measurements do not depend on equilibrium and further provides an inherent quality control, where assay problems can immediately be detected as irregularities in the binding curve. More importantly, time-resolved interaction measurements provide information about not only the affinity, but also the binding kinetics, i.e. the association and dissociation rates. This is particularly important during drug development, where it is crucial to know if the drug will have enough time to bind the target before it is cleared from the blood, and where the biological effect depends on residence time, i.e. how long a drug remains bound to its target [7]. Because of the

Abbreviations: GPCR, G protein-coupled receptor; pPYY, porcine peptide YY; hY2R, human Y2 receptor; GRPR, gastrin-releasing peptide receptor; ^{125}I, iodine-125; ^{111}In, indium-111.

* Corresponding author at: Biomedical Radiation Sciences, Rudbeck Laboratory, Uppsala University, 751 85 Uppsala, Sweden. Fax: +46 18 471 3432.

E-mail addresses: bo.xu@neuro.uu.se (B. Xu), zohreh.varasteh@pet.medchem.uu.se (Z. Varasteh), anna.orlova@pet.medchem.uu.se (A. Orlova), karl@ridgeview.eu (K. Andersson), dan.larhammar@neuro.uu.se (D. Larhammar), hanna.bjorkelund@bms.uu.se (H. Björkelund).

[1] The authors contributed equally to this work.

0006-291X/$ - see front matter © 2013 Elsevier Inc. All rights reserved.
http://dx.doi.org/10.1016/j.bbrc.2013.10.149

information-rich nature of real-time interaction data, new tools have emerged to extract additional information from such data. One example is the analytical procedure Interaction Map, which can decipher the degree of interaction heterogeneity from time resolved binding traces, to understand if a molecule binds to its target in different manners [8]. Such heterogeneity can be caused by various conformations, molecular variants or dimer states and will affect the interaction kinetics, visible through Interaction Map.

So far most real-time interaction studies have been performed in cell free systems, using e.g. the sensitive and label-free technology of surface plasmon resonance (SPR) [9,10]. However, these measurements are rarely straightforward due to difficulties in overexpression, purification and stabilization of the GPCRs [10,11]. There may further be discrepancies between the SPR results and effects in living systems, due to the lack of G-protein and stabilizing membrane components. Similar observations have been made in other systems, where large differences between SPR data and cell data were observed [12].

The aim of the present study was to establish a method for real-time measurements of interactions with GPCRs in living cells. This was conducted using the instrument LigandTracer®, which has been described in detail and validated previously for overexpressed receptors in cancer cells [13,14]. In brief, adherent cells expressing the target protein are seeded in a local part of a circular Petri dish, which is placed on an inclined, rotating support with a detector positioned over the elevated part of the dish (Fig. 1A). A buffer containing a radiolabeled molecule, e.g. a peptide or protein, is added. If the molecule binds to the target on the cells, the detector will register a peak each time the cell area passes by the detector, using a cell-free area of the dish as a reference. By following the peak height over time, a real-time binding trace is obtained. The method was originally developed for a single cell area, but after further development at least three areas can be studied in parallel, enabling e.g. comparison of binding to different cell lines (Fig. 1B).

The use of living cells in time-resolved binding assays has the potential to improve understanding of GPCRs in their true environment. Two model systems were used to evaluate the method and demonstrate proof-of-concept. In the first study, the binding of the pPYY peptide to cells expressing different degrees of the human neuropeptide receptor hY2R [15] was measured. In the second study, the interaction between the bombesin antagonist RM26 developed for medicinal imaging of cancer and the gastrin-releasing peptide receptor GRPR [16] was detected. The binding showed clear signs of interaction heterogeneity and was therefore further evaluated using Interaction Map.

2. Materials and methods

2.1. Reagents and labeling

The human peptide YY pre-labeled with ^{125}I (denoted ^{125}I-pPYY) was purchased from PerkinElmer (Product No. NEX240050UC, Waltham, MA, USA).

The bombesin antagonist analog denoted NOTA-PEG6-RM26 (NOTA-PEG6-D-Phe-Gln-Trp-Ala-Val-Gly-His-Sta-Leu-NH2 ([D-Phe6, Sta13, Leu14] bombesin) [17] was synthesized and labeled with ^{111}In (Covidien, Dublin, Ireland) as described previously [16].

2.2. Cells

The human embryonic kidney 293 cell line (HEK-293) and the human prostate cancer cell line PC3 were used in this study. The cells were grown at 37 °C, 5% CO_2, in DMEM (HEK-293) or RPMI (PC3) medium containing 10% (v/v) fetal calf serum and PEST (penicillin 100 IU/ml and streptomycin 100 μg/ml). Additionally, the DMEM medium used for the HEK-293 cells contained Amphotericin B (Life Technologies, Carlsbad, CA, USA) and the RPMI medium for PC3 contained L-Glutamine (2 mM, Biochrom Ag, Berlin, Germany).

2.3. Transfection for transient and stable protein expression of hY2R

The hY2R was inserted into a pcDNA-DEST47 expression vector. HEK-293 cells were transfected with the hY2R expression vectors using Lipofectamine 2000 and OPTI-MEM according to the instructions from the manufacturer. The same transfection procedure was used for the stable transfection. After 24 h transfection, cells with stable expression were selected using DMEM medium containing 500 μg/ml geneticin. All reagents for transfection were from Life Technologies (Carlsbad, CA, USA).

2.4. Real-time measurement of interactions with GPCR on cells in LigandTracer Grey

Approximately 1 million cells were seeded in Petri dishes (Cat. No. 172958, Nunc, Roskilde, Denmark) at least 2 days before experimental day. All binding measurements were monitored in real-time on cells using LigandTracer Grey instruments (Ridgeview Instruments AB, Vänge, Sweden), essentially as described previously [12,13,18–20].

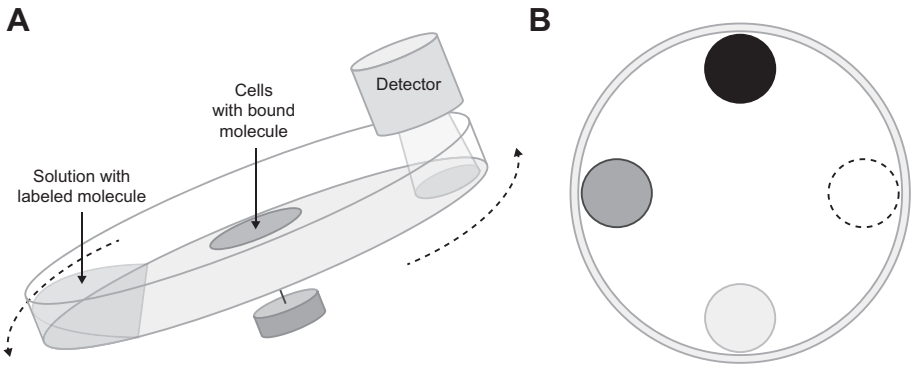

Fig. 1. Illustration of the LigandTracer technology and example of cell areas. (A) Cells are seeded in a local area of a Petri dish, which is placed on a tilted, rotating support. A solution with radiolabeled molecule is added. Radioactivity measurements are performed in the elevated area and followed over time. A target free area of the dish is used as a reference to continuously subtract the background signal. (B) In one of the experiments, the binding to three cell areas were monitored simultaneously: stably hY2R-transfected HEK-293 cells (black area), transiently transfected HEK-293 cells (dark grey area) and wild-type HEK-293 cells (light grey area). A plastic area (dashed circle) was kept cell free, used for background subtraction.

The binding of 300 pM ^{125}I-pPYY to stably expressed hY2R on transfected HEK-293 cells was measured for 5–6 h. The labeled peptide was then replaced with fresh medium, and the dissociation was followed over-night. In another measurement, the binding of 900 pM ^{125}I-pPYY was monitored to stably hY2R-transfected HEK-293, transiently hY2R-transfected HEK-293 and wild-type HEK-293 simultaneously as shown in Fig. 1 B.

The binding of 0.3 and 10 nM ^{111}In-NOTA-PEG6-RM26 was monitored for 2.5 and 1.5 h respectively, followed by a dissociation measurement over-night.

All measurements were conducted at room temperature. Corrections for nuclide decay ($t_{1/2}$ = 60 days for ^{125}I and $t_{1/2}$ = 2.8 days for ^{111}In) were done automatically in the software controlling the instrument.

2.5. Kinetic evaluation in TraceDrawer

Data was analyzed using TraceDrawer 1.5 (Ridgeview Instruments AB, Vänge, Sweden), by fitting the curves to the One-to-one kinetic model.

2.6. Estimation of interaction heterogeneity using Interaction Map

The heterogeneity of the data for GRPR was analyzed using the mathematical method Interaction Map (Ridgeview Diagnostics AB, Uppsala, Sweden), which has been validated for overexpressed surface receptors as thoroughly described previously [8,21].

The main assumption of the method is that the binding of a molecule to a target can be expressed as a sum of monovalent interactions [22,23], each having a unique combination of association rate constant k_a and dissociation rate constant k_d, and a weighting parameter W describing the contribution to the measured curve.

$$\text{Measured Curve} = \Sigma_{i=1}^{n}\Sigma_{i=1}^{m}\left[W_{ij} \times \text{Curve Component } (\text{conc}, k_a^i, k_d^j)\right]$$

This results in a two-dimensional distribution of k_a and k_d, representing the recognition and the stability of the complex, where each peak in this on–off like plot [24] corresponds to a contributing interaction of the measured curve.

3. Results

The interaction of ^{125}I-labeled pPYY with hY2R on HEK-293 cells was monitored continuously for 20 h. After 5 h of incubation the signal continued to increase, meaning that equilibrium had not yet been reached (Fig. 2A, black curve). Upon removal of the peptide solution after 5.5 h, the signal immediately started to decrease and most of the bound ^{125}I-pPYY dissociated from hY2R over the course of 15 h. The data fitted well to the one-to-one kinetic model, describing one type of molecule binding to one type of target (Fig. 2A, grey curve). According to the results of the curve fit, the interaction had an association rate constant, k_a, of $5.0 \times 10^5\ M^{-1}\ s^{-1}$ and a dissociation rate constant, k_d, of $5.1 \times 10^{-5}\ s^{-1}$. The dissociation constant, K_D (=k_d/k_a), corresponds to the affinity of the interaction and was 102 pM.

Measurement during continuous exposure to the peptide radioligand ^{125}I-pPYY for a longer period of time were performed using three different lines of HEK-293 cells: cells with a stable expression of hY2R (Fig. 2B, black solid line), cells with a transient expression of hY2R (Fig. 2B, black dashed line) and wild-type cells (Fig. 2B, grey solid line). The stable cell line produced the highest signal and the wild-type cells the lowest.

In another series of experiments, increasing concentrations of the ^{111}In-labeled bombesin antagonist (^{111}In-NOTA-PEG6-RM26) were stepwise added to PC3 cells expressing GRPR (Fig. 3A). The association rate was relatively slow when 0.3 nM concentration was used, but quickly reached equilibrium with the higher concentration (10 nM). Judging from the dissociation part of the curve, the interaction contained a fast dissociation component, observed as a quick signal decrease after ^{111}In-NOTA-PEG6-RM26 had been removed, followed by a subsequent slower dissociating component. This type of interaction behavior resulted in a poor fit to the one-to-one kinetic model (data not shown), suggesting that the interaction is not homogenous and that more than one type of interaction occurred simultaneously. The real-time interaction data were analyzed with the Interaction Map method. Both measurements resulted in similar Interaction Maps and are represented in Fig. 3B. Two peaks were visible, indicating that the interaction curve depicts the sum of two parallel interaction types. The interactions differed in association rate (k_a) but more evidently in dissociation rate (k_d). The contributions of the peaks are represented by their darkness and were calculated as the percentage of the weight factors (W_{ij}) for the pixels of the peak in comparison to the sum of all weight factors (Table 1). Interaction i had a higher affinity and contributed to approximately 75% of the signal height of the measured curves. The lower affinity interaction ii contributed to 25% of the curve signal and had a faster dissociation rate (higher k_d), explaining the quick signal drop when radiolabeled ligand was removed.

4. Discussion

In this paper, we explore the possibility of performing real-time measurement of ligand-GPCR interactions on cells by applying the method on two model systems. This was conducted using the

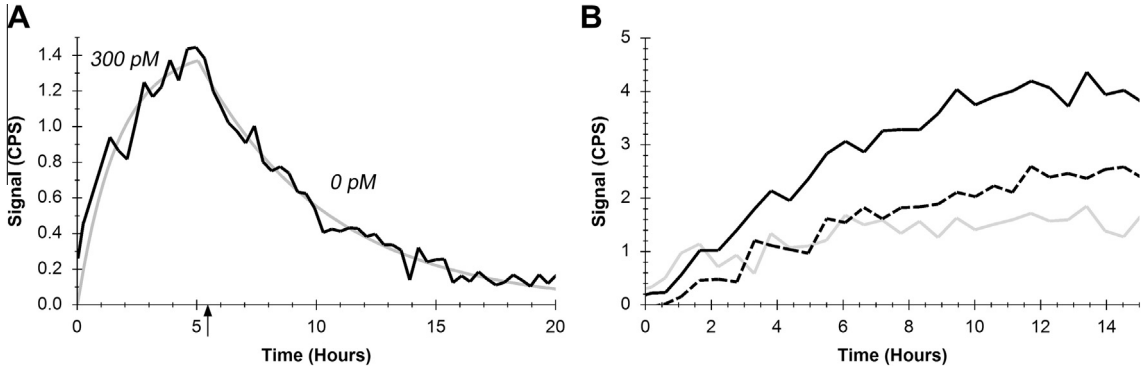

Fig. 2. Real-time binding data of the ^{125}I-pPYY–hY2R interaction. (A) Binding of ^{125}I-pPYY (300 pM) to stably hY2R-transfected HEK-293 cells (black). The arrow indicates removal of ligand, i.e. the start of the dissociation measurement. The data was fitted to a one-to-one interaction model using TraceDrawer 1.5 (grey). (B) Binding of 900 pM ^{125}I-pPYY to transiently hY2R-transfected HEK-293 cells (black solid line), stably hY2R-transfected HEK-293 cells (black dashed line) and wt HEK-293 cells (grey solid line).

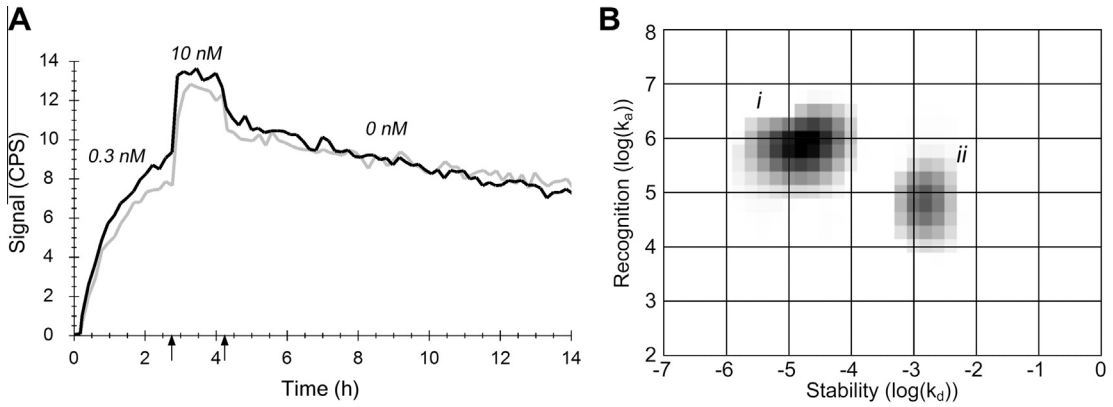

Fig. 3. Real-time binding data and Interaction Map of the ^{111}In-NOTA-PEG6-RM26–GRPR interaction. (A) Binding of the bombesin antagonist ^{111}In-NOTA-PEG6-RM26 (0.3 and 10 nM) to GRPRs on PC3 cells, followed by a dissociation measurement in which the ^{111}In-NOTA-PEG6-RM26 solution had been replaced with complete medium. Data is presented as duplicates, measured in separate dishes during the same day (grey, black). The arrows indicate the concentration increase and the start of the dissociation measurement. (B) Interaction Map, calculated from the black curve of (A).The map shows that there are two parallel interactions present, i and ii, with different kinetic constants k_a and k_d. Peak i is darker, representing a stronger contribution, and has a higher recognition (k_a) and stability (k_d), thus higher affinity. The Interaction Map calculated from the grey curve of (A) was similar (data not shown).

Table 1
Summary of Interaction Map data.

Interaction	k_a (M^{-1} s^{-1})	k_d (s^{-1})	K_D (M)	Weight (%)
i	$(5.9 \pm 0.9) \times 10^5$	$(1.4 \pm 0.2) \times 10^{-5}$	$(24.2 \pm 0.2) \times 10^{-12}$	73.4 ± 4.0
ii	$(2.4 \pm 1.8) \times 10^5$	$(2.1 \pm 0.7) \times 10^{-3}$	$(15.6 \pm 13.4) \times 10^{-9}$	25.2 ± 3.7

Kinetic parameters of peak i and ii in the Interaction Maps calculated for ^{111}In-NOTA-PEG6-RM26 from the curves of Fig. 3A. Data is presented as average ± the distribution, i.e. (maximum value − minimum value)/2.

LigandTracer technology, for which GPCR is a completely novel application. The method was proven functional for both systems, indicating that it may be generally applicable. Real-time detection of ligand-GPCR interactions are known to be difficult, primarily because such measurements are typically performed with SPR which requires expression, purification and stabilization of the receptors. By instead detecting the binding of ligand to cell associated receptors, most of these complicated steps are avoided. Additionally, GPCRs expressed on living cells may be a more relevant representation of the receptors in their true environment.

The interaction between 300 pM ^{125}I-pPYY and the transfected HEK-293 cells expressing hY2R was slow, with a time to equilibrium of more than 5 h (Fig. 2A). Slow association rates of this kind must be taken into account when performing end-point assays, which typically require that equilibrium is reached. Too short incubation times will result in inaccurate data, increasing the risk of drawing invalid conclusions about the biological system. Using higher concentrations of the molecule in solution will speed up the interaction and may be an alternative to longer incubations.

When comparing the interaction of ^{125}I-pPYY to hY2R on wild-type HEK-293 cells and transfected HEK-293 cells, a weak binding to the wild-type cells was observed (Fig. 2B). This was likely an unspecific binding, as corroborated by the different curve shape of the wild-type cells. For the two transfected cell types, the signal continued to increase over many hours, similar to the data of Fig. 2A, but for the wild-type cells the signal rapidly increased and then remained relatively stable throughout the run.

There are different possible explanations to why two types of interactions were present for the bombesin analog on PC3 cells (Fig. 3). It is possible that the two interactions correspond to the antagonist binding different conformations of the GPCR. These conformations may be constantly present on the cell surface, or the result of a conformation change occurring after ^{111}In-NOTA-PEG6-RM26 has bound. In the latter case, one would expect that the association rate would be the same for both interactions (corresponding to the antagonist binding the inactive state) and that the different dissociation rates corresponds to ^{111}In-NOTA-PEG6-RM26 detaching from either the inactive or active state. Since the differences in association rates were rather small it is difficult to exclude either of the two hypotheses. Other explanations are also possible, such as post-translational modifications.

The use of real-time binding curves to understand interaction heterogeneity is relatively new, but intriguing. This type of analysis may be particularly important for GPCRs, since the dynamics of the receptors are known but not completely understood. Studies with other receptor systems have shown that Interaction Map data in combination with a few complementary methods can provide new information about receptor properties, such as conformational changes and dimerization [21,25]. Similar measurements would be valuable for GPCRs as well, but were beyond the scope of this paper. For example, it would be of interest to study whether the interaction kinetics varies between cells expressing different proportions of GPCRs and G-proteins. Additionally, measuring the uptake of the molecule for various time lengths before switching to dissociation may solve the issue of whether different conformations are always present or only triggered upon binding. If a shorter incubation time would shift the contribution of the two interactions in Fig. 3B, this would suggest that GRPR requires some time before one of the conformation states is created, i.e. the ligand binding will lead to a change in the receptor's conformation. In this study only the GRPR interaction was evaluated further with Interaction Map. This was because the hY2R data fitted the one-to-one data well but also due to the slow association rate of this ligand-receptor pair. The developers of Interaction Map recommend that for proper analysis the binding data should contain (a) at least two different concentrations, (b) measurement of each concentration for long enough to get a clear curvature, (c) a dissociation phase with visible curvature. Using a slow binder such as hPYY

would require many hours (>30 h) of measurement to produce this kind of data, which may be detrimental for the peptide or the cells.

In conclusion, this paper presents a novel method for measuring real-time interactions with GPCRs on cells which provides information about affinity and binding kinetics in a living system, without the need of purification and stabilization of the receptors. The assay does not require that the interaction reaches equilibrium to produce accurate results. Because the binding is continuously monitored throughout the experiment the number of blind-spots is reduced. With advanced analysis tools such as Interaction Map the real-time data can be further evaluated to understand the complexity of living cells, displayed as e.g. interaction heterogeneity. Applying this method in GPCR-related research may improve the understanding of both the ligand interaction per se and the subsequent signaling events.

Acknowledgments

The authors would like to acknowledge Ph.D. G. Lindeberg, Department of Medicinal Chemistry, Uppsala University, Sweden, for synthesis of NOTA-PEG6-RM26.

This work was supported by grants from the Swedish Research Council.

References

[1] J.A. Salon, D.T. Lodowski, K. Palczewski, The significance of G protein-coupled receptor crystallography for drug discovery, Pharmacol. Rev. 63 (2011) 901–937.

[2] I.S. Moreira, Structural features of the G-protein/GPCR interactions, Biochim. Biophys. Acta (2013) [Epub ahead of print], <http://www.ncbi.nlm.nih.gov/pubmed/24016604>.

[3] S. Galandrin, G. Oligny-Longpre, M. Bouvier, The evasive nature of drug efficacy: implications for drug discovery, Trends Pharmacol. Sci. 28 (2007) 423–430.

[4] J.D. Urban, W.P. Clarke, M. von Zastrow, D.E. Nichols, B. Kobilka, H. Weinstein, J.A. Javitch, B.L. Roth, A. Christopoulos, P.M. Sexton, K.J. Miller, M. Spedding, R.B. Mailman, Functional selectivity and classical concepts of quantitative pharmacology, J. Pharmacol. Exp. Ther. 320 (2007) 1–13.

[5] E.C. Hulme, M.A. Trevethick, Ligand binding assays at equilibrium: validation and interpretation, Br. J. Pharmacol. 161 (2010) 1219–1237.

[6] K. Andersson, H. Björkelund, M. Malmqvist, Antibody-antigen interactions: what is the required time to equilibrium?, Nat Prec. (2010). <http://precedings.nature.com/documents/5218/version/1/files/npre20105218-1.pdf>.

[7] R.A. Copeland, D.L. Pompliano, T.D. Meek, Drug-target residence time and its implications for lead optimization, Nat. Rev. Drug Discov. 5 (2006) 730–739.

[8] D. Altschuh, H. Bjorkelund, J. Strandgard, L. Choulier, M. Malmqvist, K. Andersson, Deciphering complex protein interaction kinetics using Interaction Map, Biochem. Biophys. Res. Commun. 428 (2012) 74–79.

[9] I. Navratilova, J. Besnard, A.L. Hopkins, Screening for GPCR ligands using surface plasmon resonance, ACS Med. Chem. Lett. 2 (2011) 549–554.

[10] P.J. Harding, T.C. Hadingham, J.M. McDonnell, A. Watts, Direct analysis of a GPCR-agonist interaction by surface plasmon resonance, Eur. Biophys. J. 35 (2006) 709–712.

[11] R. Grisshammer, Purification of recombinant G-protein-coupled receptors, Methods Enzymol. 463 (2009) 631–645.

[12] J. Nilvebrant, G. Kuku, H. Björkelund, M. Nestor, Selection and in vitro characterization of human CD44v6-binding antibody fragments, Biotechnol. Appl. Biochem. 59 (2012) 367–380.

[13] H. Bjorke, K. Andersson, Automated, high-resolution cellular retention and uptake studies in vitro, Appl. Radiat. Isot. 64 (2006) 901–905.

[14] H. Bjorke, K. Andersson, Measuring the affinity of a radioligand with its receptor using a rotating cell dish with in situ reference area, Appl. Radiat. Isot. 64 (2006) 32–37.

[15] B. Xu, G. Sundstrom, S. Kuraku, I. Lundell, D. Larhammar, Cloning and pharmacological characterization of the neuropeptide Y receptor Y5 in the sea lamprey, *Petromyzon marinus*, Peptides 39 (2013) 64–70.

[16] Z. Varasteh, I. Velikyan, G. Lindeberg, J. Sorensen, M. Larhed, M. Sandstrom, R.K. Selvaraju, J. Malmberg, V. Tolmachev, A. Orlova, Synthesis and characterization of a high-affinity NOTA-conjugated bombesin antagonist for GRPR-targeted tumor imaging, Bioconjug. Chem. (2013) (Epub ahead of print).

[17] R. Mansi, X. Wang, F. Forrer, B. Waser, R. Cescato, K. Graham, S. Borkowski, J.C. Reubi, H.R. Maecke, Development of a potent DOTA-conjugated bombesin antagonist for targeting GRPR-positive tumours, Eur. J. Nucl. Med. Mol. Imaging 38 (2011) 97–107.

[18] M. Nestor, K. Andersson, H. Lundqvist, Characterization of ^{111}In and 177Lu-labeled antibodies binding to CD44v6 using a novel automated radioimmunoassay, J. Mol. Recognit. 21 (2008) 179–183.

[19] G. Malviya, E.F. de Vries, R.A. Dierckx, A. Signore, Synthesis and evaluation of 99mTc-labelled monoclonal antibody 1D09C3 for molecular imaging of major histocompatibility complex class II protein expression, Mol. Imaging Biol. 13 (2011) 930–939.

[20] L. Ekerljung, J. Lennartsson, L. Gedda, The HER2-binding affibody molecule (Z(HER2ratio342))(2) increases radiosensitivity in SKBR-3 cells, PloS One 7 (2012) e49579.

[21] H. Bjorkelund, L. Gedda, P. Barta, M. Malmqvist, K. Andersson, Gefitinib induces epidermal growth factor receptor dimers which alters the interaction characteristics with (1)(2)(5)I-EGF, PloS One 6 (2011) e24739.

[22] J. Svitel, A. Balbo, R.A. Mariuzza, N.R. Gonzales, P. Schuck, Combined affinity and rate constant distributions of ligand populations from experimental surface binding kinetics and equilibria, Biophys. J. 84 (2003) 4062–4077.

[23] K. Andersson, M. Malmqvist, Method for the analysis of solid biological objects, Patent application WO 2010033069 (2008).

[24] P.O. Markgren, W. Schaal, M. Hamalainen, A. Karlen, A. Hallberg, B. Samuelsson, U.H. Danielson, Relationships between structure and interaction kinetics for HIV-1 protease inhibitors, J. Med. Chem. 45 (2002) 5430–5439.

[25] H. Björkelund, L. Gedda, M. Malmqvist, K. Andersson, Resolving the EGF-EGFR interaction characteristics through a multiple-temperature, multiple-inhibitor, real-time interaction analysis approach, Mol. Clin. Oncol. 1 (2013) 343–352.